Preliminary Communication

For reprint orders, please contact: reprints@futuremedicine.com

Nanomedicine

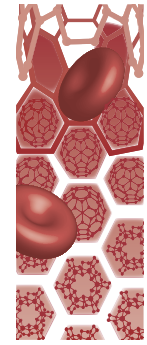

The role of formulation approaches in presenting targeting ligands on lipid nanoparticles

Robert Castro[1], Elizabeth Aisenbrey[2] & Liwei Hui*[,1]

[1]EMD Millipore Corporation, Temecula, CA 92590, USA

[2]Sigma-Aldrich Co. LLC, Milwaukee, WI 53209, USA

*Author for correspondence: liwei.hui@milliporesigma.com

Aims: The density of functional ligands on lipid nanoparticles (LNPs) greatly determined its capability of postfunctionalization and targetability for the applications of personalized nanomedicine and drug/gene delivery. This work is to investigate whether and how formulation methods influence the presentation of surface ligands. **Methods:** Biotin-modified LNPs as a functional LNP model were synthesized by four different formulation methods. The biotin ligand density and targetability of biotin-LNPs were evaluated and compared. **Results:** Both the ligand density and targetability of biotin-LNPs formulated by four different formulation methods exhibited a similar trend: homogenization > extrusion > wave-shaped micromixer ≈ Y-shaped micromixer. **Conclusion:** Formulation methods could modulate the presentation of targeting ligands on LNPs, which could guide future formulation screening and nanomedicine engineering.

First draft submitted: 25 February 2023; Accepted for publication: 6 April 2023; Published online: 18 May 2023

Keywords: drug delivery • extrusion • formulation • functionalization • homogenization • liposome • microfluidic mixing • nanomedicine • targeting

Lipid nanoparticle (LNP) has emerged as a critical component and vehicle in delivering a variety of ingredients and drugs [1,2]. Since the first LNP-based nanomedicine, Active Ingredient (Active Ingredient loaded in LNPs), launched in 1995, there have been more than 30 lipid-based nanomedicines approved and used in the clinic [3]. In addition to their success in the pharmaceutical industry, LNPs also show tremendous potentials in broad fields, such as medical imaging [4], cosmetics [5], agriculture [6] and nanoreactors [7].

The progress in LNPs is not only driven by the synthesis of novel, degradable and intelligent lipids, but is also driven by surface modification techniques that can upgrade the function and clinical translation of LNPs, especially in precision nanomedicine applications [8,9]. Compared with bare LNPs, surface modification can 1) inhibit nonspecific interactions with intrinsic physiological molecules (e.g., PEG modification to inhibit the formation of protein corona); 2) contribute to active targeting against specific organelles, cells and tissues (e.g., anchoring targeting ligands to recognize cancerous cells) and 3) allow for construction of nanovaccines (e.g., virus-like nanoparticles) [10,11]. In past years, the boom of phage-display techniques and high-throughput screening greatly promoted the discovery of targeting peptides and oligonucleotides and advanced the engineering of active targeting LNPs, as well as personalized ones [12,13]. However, the ability to precisely control and modulate the presentation of surface ligands and functional groups on LNPs remains an unresolved challenge.

In general, there are two approaches to control the density of surface ligands. One is by changing the feed ratio of functional lipids relative to the total lipid mixture, and the other is by implementing site-specific surface conjugation. Chen *et al.* found there is an optimal ligand density on the surface of LNPs – 0.5–2.0 ligands/100 nm^2 for folate, 0.7 ligands/100 nm^2 for transferrin and 0.2 ligands/100 nm^2 for HER2-antibody, for instance – for target cell recognition [14]. However, increasing the feed ratio of functional lipids did not further increase the targetability of surface ligands [15]. Alternatively, site-specific conjugation relies on unique and definable reaction sites, such as binding peptides and enzyme-catalyzed conjugation. The activity of site-specific conjugation is dependent on

Future Medicine

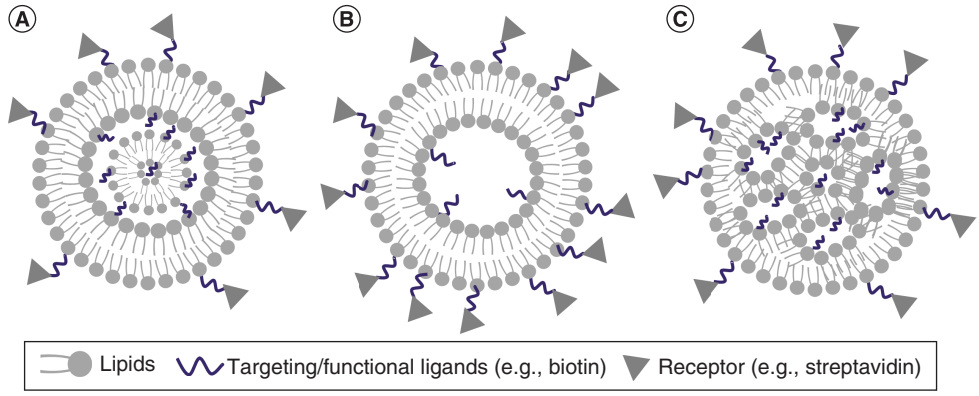

D

Method	Potential structure	Ligand density
Extrusion	(a) Multilaminar	++
Homogenization	(b) Bilayer	+++
Microfluidic mixing	(c) Close-packed	+

Figure 1. Scheme of presenting ligands on lipid nanoparticles and formulation approaches. (A–C) Structures of targeting LNPs (e.g., biotin-LNP) and the recognition/conjugation to targeted receptors (e.g., streptavidin). **(A)** Multilaminar structure where more than two lipid bilayers were assembled (the structure was optimally formed by extrusion method), **(B)** single lipid bilayer structure which was optimally fabricated by homogenization method where high energy could break up the multilayer barriers and induce controllable assembly and **(C)** close-packed structure where lipid islands were commonly formed and generally prepared by microfluidic methods. **(D)** Summary of formulation methods and most promising structures, as well as corresponding ligand density after formulation. LNP: Lipid nanoparticle.

orientation and yield of conjugates [16,17]. For example, Fc-binding peptides were found to selectively conjugate with Fc chains of IgG antibodies while the remaining Fab chain protruded externally to recognize antigens [18]. These studies demonstrated the feasibility to modulate the surface density of targeting ligands which presented on the surface of LNPs by ratio control and site-specific conjugations.

In this work, we explored whether formulation method modulates the presentation of targeting ligands on the surface of LNPs. Generally, LNP can be prepared by thin-film hydration approach and microfluidics approach [1]. For thin-film hydration, the size of LNP can be controlled by extrusion or by homogenization, such as ultrasonic homogenization which can disrupt the energy barrier of multilayers and induce single bilayer liposome. With microfluidics methods, the geometry of micromixer including the mixing cycles and mixing distance could greatly influence the size of LNPs and their stability [19]. Depending on the lipid and its interaction with payloads, the structure of LNPs prepared by different formulation methods can be varied, ranging from bilayer, multilaminar to closely packed (Figure 1) [20]. Theoretically, for thin-film hydration method, the multilaminar lipid membrane was formed upon hydration, and can be disrupted with high energy (e.g., homogenization); for microfluidic methods, the organic solvents (e.g., ethanol) were miscible in LNP dispersion and subsequently removed by buffer exchange, which might induce the formation of lipid islands or empty cavity within lipid shells. Therefore, at the same lipid concentration, the surface density of ligands distributed on LNPs with single bilayer structure (Figure 1B) should be higher than that distributed on LNPs with multilayer structure (Figure 1A) or close-packed structures (Figure 1C) where many ligands were shielded within the LNP core (Figure 1D). As a result, the density of accessible targeting ligands might be modulated by formulation process. However, there are few studies investigating how formulation methods influence the presentation of surface ligands, neither the structure nor surface chemistry, of functional LNPs.

Using biotin-modified lipid nanoparticles (biotin-LNPs) as a model, our results showed that functional LNPs prepared by thin-film hydration methods presented more ligands and higher targetability than LNPs prepared by microfluidics methods. Instead of feed ratio control, this work demonstrated a new approach of modulating the presentation of targeting ligands by selecting formulation methods. Though further work is required to elucidate

the underlying mechanisms, this study will contribute to the development of active targeting LNPs, as well as the screening of multifunctional and precision nanomedicines.

Materials & methods

Materials

Streptavidin (catalog no. 189730), biotin-modified lipid mix kit (catalog no. 932612), PEGlyated lipid mix kit (catalog no. 922420), ethanol (ethanol 200, anhydrous), tetramethylindocarbocyanine perchlorate (Dil) (catalog no. 468495), phosphate-buffered saline (PBS) and all culture media were purchased from Sigma-Aldrich (MI, USA). Micro BCA™ Protein Assay Kit (catalog no. 23235) was ordered from Thermo Fisher Scientific (IL, USA).

Preparation of LNPs by extrusion

For nanoparticles prepared by extrusion, one vial of lipid mix (25 mg) was hydrated with sterile ammonium sulfate buffer (240 mM; pH = 5.4) to a final lipid concentration of 25 mg/ml. The lipid mix solution was vortexed and incubated at 65°C for 1 h. The resulting lipid dispersions were subsequently subjected to seven freeze–thaw cycles and extruded through nucleopore membrane with pore size of 100 nm using mini hand extruder with thermojacket (Genizer, CA, USA). The thermojacket was connected to standard digital heated circulator to maintain the extrusion temperature at 65°C. After 21-times extrusion, the lipid solution was collected and dialyzed against PBS buffer overnight. The obtained LNPs were stored at 4°C prior to use.

Preparation of LNPs by homogenization

For nanoparticles prepared by homogenization, one vial of lipid mix (25 mg) was hydrated with sterile ammonium sulfate buffer (240 mM; pH = 5.4) to a final lipid concentration of 10 mg/ml. After vortex and incubation at 65°C for 1 h, the lipid dispersion was sonicated with ultrasonic homogenizer (Benchmark, Pulse 150, NJ, USA) to clarity (at an output power of 7.5 W for 20 min, pulse 2 s). The obtained LNPs were dialyzed against PBS buffer overnight and stored at 4°C for further use.

Preparation of LNPs by microfluidic micromixer

For nanoparticles prepared by microfluidic micromixer, one vial of lipid mixture (25 mg) was dissolved in ethanol to a final concentration of 25 mg/ml and vortexed completely until clarity. The microfluidic micromixer (NanoFabTx™ Microfluidic Nano Device kit, catalog # 911593, Sigma-Aldrich) was connected into two syringes which were controlled by syringe pumps. The flow rate of buffer phase (sterile ammonium sulfate buffer) was 250 µl/min, while that of ethanol phase (lipid mixture dispersion) was 50 µl/min. The obtained lipid dispersion was dialyzed against PBS buffer overnight and stored at 4°C for further use.

Preparation of LNPs by microfluidic NanoAssemblr

For nanoparticles prepared by NanoAssemblr Ignite (Precision Nanosystems Inc.; Vancouver, Canada), one vial of lipid mixture (25 mg) was similarly dispersed in ethanol at the final concentration of 25 mg/ml. The lipid dispersion was vortexed and dissolved completely. The total flow rate was 8 ml/min and flow rate ratio between buffer phase (sterile ammonium sulfate buffer) and ethanol phase (lipid mixture dispersion) was 3:1. The total volume was 1.5 ml with 0.15 ml initial waste and 0.05 ml final waste. The obtained lipid dispersion was dialyzed against PBS buffer overnight and stored at 4°C for further use.

Characterization of LNPs

The hydrodynamic diameter and the diameter distribution of obtained lipid dispersion were characterized with a Zetasizer (Nano-ZS90, Malvern, UK). In a sample cuvette, the lipid dispersion was diluted with PBS buffer to 0.5 mg/ml. The data were collected at room temperature with three individual scans. The reported results were averages of two independent measurements.

Conjugation of LNPs with avidin-tagged proteins

To modify LNP surface with specified streptavidin, the obtained LNP dispersion was incubated with streptavidin at a molar ratio of 1:2 (molar of biotin provided in lipid mix kits:molar of streptavidin) in PBS. After 3 h incubation, the mixture was diluted with PBS and filtrated through Amicon Ultra-0.5 Centrifugal Filter Unit (Molecular weight cut-off: 100 kDa) at 10,000× g. The conjugation mixture was washed five times with PBS. The obtained conjugation products were stored at 4°C for further use.

The conjugated streptavidin was quantified with Micro BCA™ Protein Assay Kit. Briefly, the obtained conjugation products were mixed with BCA working reagents at volume ratio of 1:1 and incubated at 60°C for 30 min. The reactants were transferred to a 96-well microplate and the absorption was measured by microplate reader (Varioskan LUX, Thermo Fisher Scientific, MA, USA) at 562 nm. The dilution of streptavidin stock solutions that was measured with the same methods was used as standard curve to calculate the concentration of conjugated streptavidin. The reported results were the average of two independent trials.

Targetability of LNPs

To further evaluate if the surface ligands of LNPs prepared by different methods could influence their targetability, the LNPs were loaded with fluorescent probes. Dil is a lipophilic dye which only shows fluorescence in lipid bilayer and represented the presence of LNPs. HeLa cells were used as a representative biotin-targeting cell. To prepare Dil-loaded LNPs, Dil in ethanol was mixed with lipid dispersions to achieve a final Dil-to-lipid molar ratio of 8% [21]. For extrusion and ultrasonic homogenization methods, the lipid mixture was dried to a thin film first, followed by hydrating with ammonium sulfate buffer. While for microfluidic micromixer and NanoAssemblr methods, Dil solution was directly mixed with lipid dispersions, followed by two-phase mixing to form LNPs.

Approximately 200,000 cells in fetal bovine serum (FBS)-supplemented DMEM medium were seeded into a 96-well microplate and incubated overnight. The cells were washed with medium once and incubated with Dil-loaded biotin-LNPs for 48 h. Subsequently, the cells were washed with sterile PBS four times. The fluorescence of obtained cells was measured by microplate reader (Varioskan LUX, Thermo Fisher Scientific) with excitation wavelength of 550 nm and emission wavelength of 585 nm. The Dil-loaded control LNPs were used as control to quantify the enhanced cell uptake capability. Each sample was performed in triplicate and the reported results were the average of two independent experiments.

Cytotoxicity of LNPs

To evaluate the biocompatibility of obtained LNPs, the cytotoxicity experiment of Cell Counting Kit-8 (catalog no. 96992, Sigma-Aldrich, MO, USA) assay was performed. HeLa cell was used as a representative mammalian cell. Approximately, 40,000 cells in FBS-supplemented DMEM medium were seeded into a 96-well microplate and incubated overnight. The medium was removed and replaced with LNPs which were diluted with FBS-supplemented DMEM medium at desired concentration. After 24 h incubation, the LNP dispersion was removed and washed with PBS buffer. Followed by the addition of Cell Counting Kit-8 reagents and incubation in 37°C incubator for 1 h, the absorption at 450 nm was read with a microplate reader (Varioskan LUX, Thermo Fisher Scientific). Each sample was performed in triplicate and the reported results were the average of two independent trials.

Results

LNP was prepared by four common methods, including thin-film hydration-based extrusion and ultrasonic homogenization, and microfluidic mixing with wave-shape micromixer and with Y-shape NanoAssemblr mixer. Biotin-modified LNPs were chosen as a functional LNP model. To make a comprehensive comparison, the size of formulated LNPs was modulated to approximately 100 nm. To do so, proper formulation conditions were screened. For thin-film hydration methods, the pore size of the extrusion membrane was 100 nm, while the ultrasonic homogenization duration and power were optimized to 20 mins and 7.5 W, respectively. As for microfluidic mixing, the flow rate of the ethanol phase and flow rate ratio of ethanol-to-buffer phase were optimized to 50 µl/min and 1:5 for the wave-shape micromixer, and 2 ml/min and 1:3, respectively, for the Y-shape NanoAssemblr. Other parameters such as different ultrasonic power, duration or flow rate resulted in larger size and broader diameter distribution. As shown in Figure 2, the hydrodynamic diameter of approximately 110 nm was achieved for the four preparation methods. The polydispersity index (PDI) was less than 0.25 for each method, suggesting a narrow distribution of as-obtained LNPs, especially extrusion which controlled the size of LNPs at individual nanoparticle level exhibiting PDI of less than 0.1. Meanwhile, LNPs formulated by four methods showed zeta potentials of around -27 mV.

The density of biotin ligands presented on the surface of the LNPs was quantified by conjugated streptavidin. Streptavidin is one kind of avidin protein which can specifically conjugate with biotin. After conjugation, the concentration of conjugated streptavidin was measured by BCA kit. As shown in Figure 3, the density of biotin presented on extrusion-formulated LNPs was 6.89 ± 0.75 µmol per 10 mg lipids, lower than the 11.93 ± 1.95 µmol

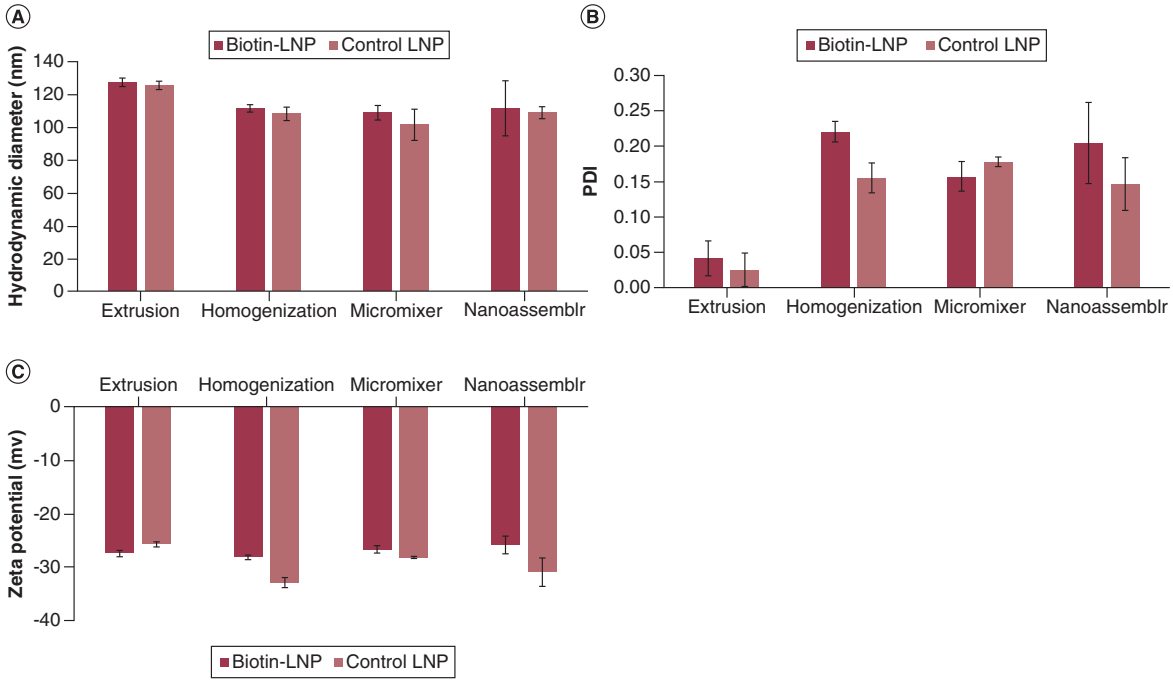

Figure 2. Characterization of biotin-lipid nanoparticle and lipid nanoparticle without biotin modification (control lipid nanoparticle) formulated by thin-film hydration based extrusion or homogenization method and microfluidic based micromixer or NanoAssemblr method. (A) Hydrodynamic diameter, **(B)** PDI and **(C)** zeta-potential of biotin-LNP and control LNP. The reported data are the average of two independent trials. Data points are reported as mean ± standard deviation.
Biotin-LNP: Biotin-modified lipid nanoparticle; LNP: Lipid nanoparticle; PDI: Polydispersity index.

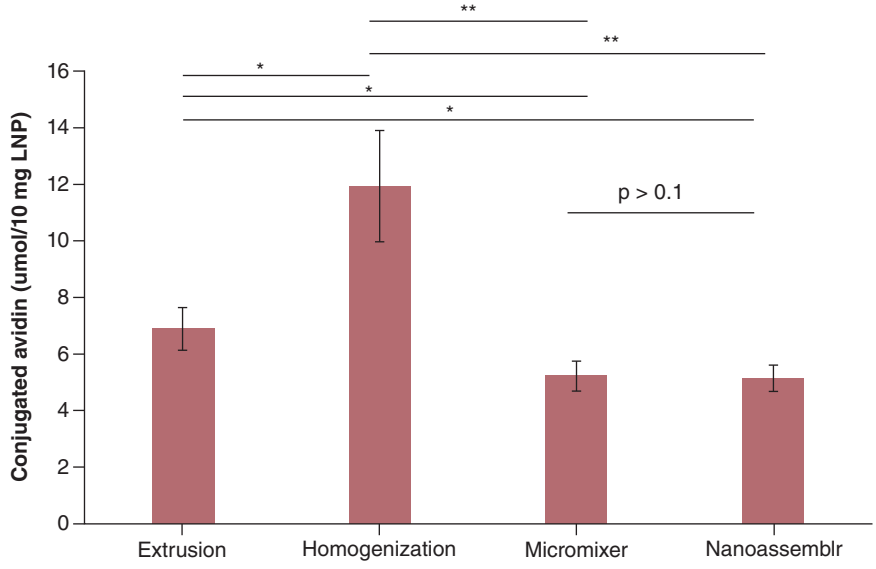

Figure 3. The surface density of biotin ligands which were quantified by the amount of conjugated streptavidin. *$p < 0.05$ and **$p < 0.01$, which suggested statistical difference and significant difference; $p > 0.1$ suggested no statistical difference. The reported data are the average of two independent trials and reported as mean ± standard deviation.

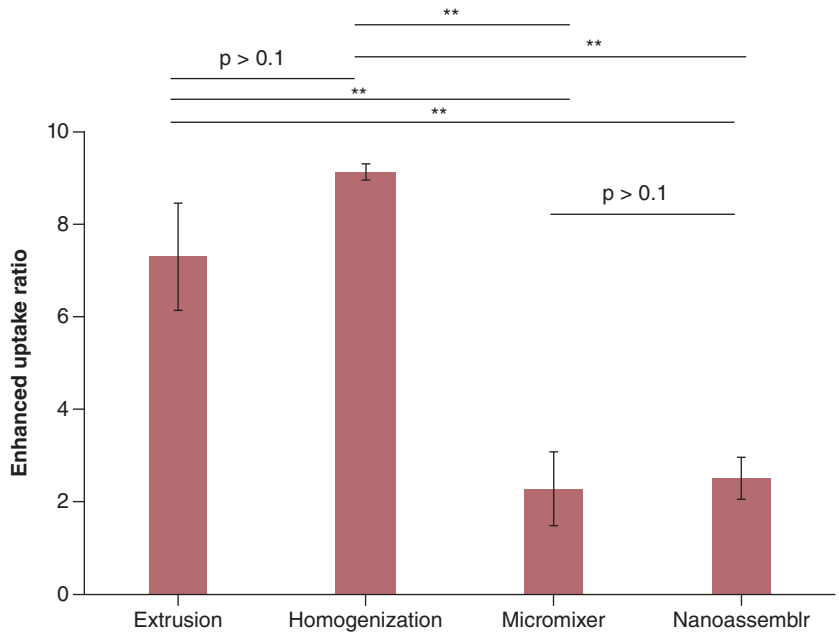

Figure 4. Targetability of biotin-lipid nanoparticles. To calculate the enhanced cell uptake ratio, the cell uptake of Dil-loaded biotin-LNP was divided by Dil-loaded nonmodified LNP (Dil-loaded control LNP).
**$p < 0.01$, which suggested significant difference; $p > 0.1$ suggested no statistical difference. The reported data are the average of two independent trials and reported as mean ± standard deviation.
LNP: Lipid nanoparticle.

per 10 mg lipid of biotin that was presented on the homogenization-formulated LNPs. In contrast, the density of biotin presented on micromixer-formulated LNPs was 5.22 ± 0.52 μmol per 10 mg lipids, similar to the 5.14 ± 0.46 μmol per 10 mg lipids of biotin presented on NanoAssemblr-formulated LNPs.

In addition to influencing the surface chemistry of postconjugation with targeting ligands, the surface density of ligands is greatly correlated with its targetability. To evaluate this hypothesis, the recognition and internalization of biotin-LNPs against target cells was tested. Biotin-LNPs were loaded with fluorescent hydrophobic dye Dil. Dil only exhibited fluorescence within lipid bilayers, which indicated the presence of LNPs. After incubation with target cells (i.e., HeLa cells), the uptake of LNPs was measured directly by the fluorescence of Dil. LNPs without biotin modification (PEGlyated LNPs as control LNPs) were used as a control to calculate the enhanced cell uptake that was induced by biotin targeting (Figure 4). Interestingly, the enhanced cell uptake ratio of LNPs formulated by extrusion method was 7.30 ± 1.15, lower than the 9.13 ± 0.17 of LNPs formulated by ultrasonic homogenization method. Meanwhile, enhanced cell uptake ratio of LNPs formulated with micromixer method was 2.29 ± 0.79, close to the 2.51 ± 0.45 of LNPs formulated with NanoAssemblr method.

To test that the difference of enhanced cell uptake was induced by the density of surface ligands rather than the cytotoxicity of LNPs, the cytotoxicity of biotin-LNPs was evaluated. HeLa cell was used as a mammalian cell model. As shown in Figure 5, the cell viability of all biotin-LNP prepared by the four different methods was above 90% at LNP concentrations of 1 mg/ml. This data suggested that the as-obtained biotin-LNPs are biocompatible and do not cause mammalian cell death.

Discussion

Biotin-modified LNP was chosen as a functional LNP model. First, biotin as a functional group is stable during all the formulation process. Second, the density of active biotin ligands can be characterized with avidin protein that specifically conjugates with biotin [22]. Lastly, the biotin moiety, as a representative targeting ligand, can also be used to selectively target specific biotin-transporter overexpressed cell lines [23,24]. The data of hydrodynamic diameter, PDI and zeta potential of LNPs suggested the LNPs formulated by the four methods were comparable to each other.

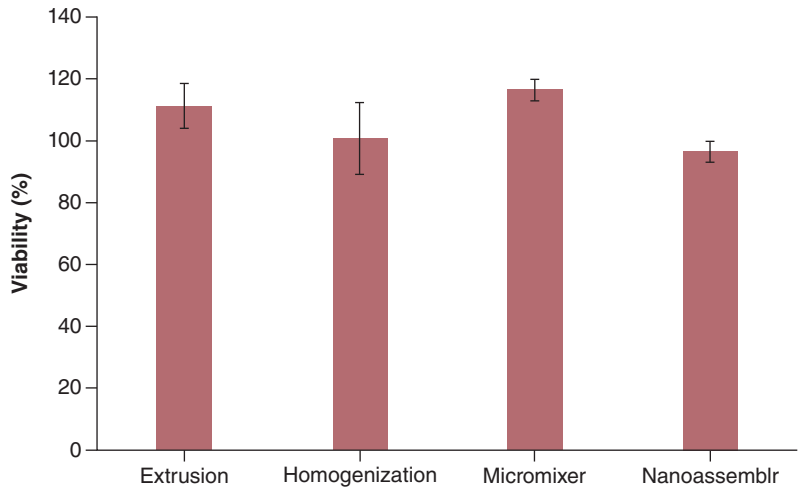

Figure 5. Cytotoxicity of biotin-lipid nanoparticles. All four kinds of biotin-LNP did not kill HeLa cells. The reported data are the average of two independent trials and reported as mean ± standard deviation.
Biotin-LNP: Biotin-modified lipid nanoparticle.

However, biotin density presented on homogenization-formulated LNPs was higher than extrusion-formulated LNPs, followed by micromixer and NanoAssemblr-formulated LNPs. Meanwhile, this ligand density trend was consistent with targetability difference presented by cell-uptake data, where enhanced cell uptake of LNPs formulated by thin-film hydration methods was also higher than that formulated by microfluidic mixing methods. The similarity of ligand density and targetability between micromixer-formulated biotin-LNPs and NanoAssemblr-formulated biotin-LNPs suggested the geometry of microfluidics did not influence the formulation process of biotin-LNPs. This order is consistent with our hypothesis (Figure 1) that targeting LNPs prepared by different methods would present different ligand densities on the surface of LNPs, probably due to the formation of different nanostructures. Homogenization could optimally generate single bilayer nanostructures, which could present more targeting ligands. In contrast, either the multilaminar or close-packed lipid island structures commonly formulated by extrusion or microfluidic mixing would shield the ligands inside the nanostructure and make it inaccessible for conjugation or recognition.

The structure of LNPs is influenced by the structure of lipids (inverted cone, cylinder and cone) and interaction between lipids (electrostatic interaction, hydrophobic interactions), as well as buffer environment (ions such as Na^+, Ca^{2+}) [25]. Incorporating cationic lipids or materials could induce the transformation of small unilamellar vesicles into micrometer-sized multilamellar vesicles, or membrane fusion between lipid bilayers [26,27]. To elucidate the underlying mechanism, direct proof of structure characterization on LNP is the first step, which requires advanced characterization techniques, such as cryogenic transmission electron microscopy, scanning electron microscopy and small-angle x-ray scattering. Moreover, single-particle analysis of surface ligands including their distribution and orientations could help disclose why other ligands are inaccessible. We hope this work here would motivate structural biologists or analytical chemists who have access to those resources or simulation capabilities to help advance our understanding on targeting LNPs, as well as other targeting nanomedicines.

In addition, our targetability assays showed compared with control LNPs without the incorporation of biotin ligands, biotin-LNPs could uptake more than two-times of dye-loaded LNPs, even nine-times for the biotin-LNPs formulated by homogenization methods. This data suggested the capability of biotin-LNPs to recognize and be uptaken by receptor-specific cells. For *in vivo* applications, this kind of active targeting could ensure the consistency between *in vitro* assays and *in vivo* trials, which were different from passive targeting systems where the system circulation and microenvironment of diseases were more relevant [1]. More studies to deliver specific drugs or provide detailed pharmacokinetic and pharmacodynamic profiles are needed and might be also personalized for different active targeting LNPs which are inherited from different recognition and targeting mechanisms.

Conclusion

In summary, we studied targeting LNPs formulated by four different methods. Our results showed that biotin-modified LNPs formulated by thin-film hydration methods presented both higher surface density of biotin ligands and targetability than those of biotin-LNP formulated by microfluidic mixing methods. This trend was consistent with our hypothesis that the formulation process could influence the presentation of targeting ligands. Future studies to elucidate the underlying mechanisms especially the structure characterization and single particle analysis for LNPs are called out. Our preliminary data highlighted the importance of formulation methods on optimizing targetability or conjugation efficiency of targeting LNPs, which undoubtedly provides guidelines for formulation screening and nanomedicine engineering.

Summary points

- Lipid nanoparticles (LNPs) with similar size and zeta potential could be obtained by selecting the conditions of different formulation methods including extrusion, homogenization or different micromixers.
- The ligands presenting on targeting LNPs were influenced by the formulation process.
- The biotin density presented on extrusion-based LNPs and homogenization-based LNPs was higher than that of microfluidic mixing-based LNPs.
- Targetability of targeting LNPs formulated by extrusion or homogenization methods was higher than that of targeting LNPs formulated by microfluidic mixing.
- The geometry of microfluidic mixer did not influence the presentation of targeting ligands.
- The homogenization could help achieve the optimal ligand density on the surface of targeting LNPs.
- The biotin-LNPs were biocompatible.
- The biotin-LNP could encapsulate hydrophobic molecules, such as lipophilic dyes.

Author contributions

R Castro investigated and performed the experiments and analyzed the data. E Aisenbrey reviewed the data and revised the manuscript. L Hui conceptualized, supervised and wrote the paper.

Acknowledgment

We thank P Gao and A Raw for the suggestions and support.

Financial & competing interests disclosure

R Castro and L Hui are employed by EMD Millipore Corporation, and E Aisenbrey is employed by Sigma-Aldrich Co. LLC, both affiliates of Merck, during the development of this work. The authors have no other relevant affiliations or financial involvement with any organization or entity with a financial interest in or financial conflict with the subject matter or materials discussed in the manuscript apart from those disclosed.

No writing assistance was utilized in the production of this manuscript.

References

Papers of special note have been highlighted as: • of interest; •• of considerable interest

1. Menon I, Zaroudi M, Zhang Y, Aisenbrey E, Hui L. Fabrication of active targeting lipid nanoparticles: challenges and perspectives. *Mater. Today Adv.* 16, 100299 (2022).

•• **Reviewed how to formulate active targeting lipid nanoparticles (LNPs) including one-pot assembly with functional lipids and postfunctionalization of functional LNPs.**

2. Hou X, Zaks T, Langer R, Dong Y. Lipid nanoparticles for mRNA delivery. *Nat. Rev. Mater.* 6(12), 1078–1094 (2021).
3. Shi J, Kantoff PW, Wooster R, Farokhzad OC. Cancer nanomedicine: progress, challenges and opportunities. *Nat. Rev. Cancer.* 17(1), 20–37 (2017).
4. Namiki Y, Fuchigami T, Tada N *et al.* Nanomedicine for cancer: lipid-based nanostructures for drug delivery and monitoring. *Acc. Chem. Res.* 44(10), 1080–1093 (2011).
5. Ahmad J. Lipid nanoparticles based cosmetics with potential application in alleviating skin disorders. *Cosmetics* 8(3), 84 (2021).
6. Karny A, Zinger A, Kajal A, Shainsky-Roitman J, Schroeder A. Therapeutic nanoparticles penetrate leaves and deliver nutrients to agricultural crops. *Sci. Rep.* 8(1), 7589 (2018).
7. Koyani R, Pérez-Robles J, Cadena-Nava RD, Vazquez-Duhalt R. Biomaterial-based nanoreactors, an alternative for enzyme delivery. *Nanotechnol. Rev.* 6(5), 405–419 (2017).

8. Mitchell MJ, Billingsley MM, Haley RM *et al.* Engineering precision nanoparticles for drug delivery. *Nat. Rev. Drug Discov.* 20(2), 101–124 (2021).
9. Dilliard SA, Siegwart DJ. Passive, active and endogenous organ-targeted lipid and polymer nanoparticles for delivery of genetic drugs. *Nat. Rev. Mater.* 8(4), 1–19 (2023).
10. Dammes N, Goldsmith M, Ramishetti S *et al.* Conformation-sensitive targeting of lipid nanoparticles for RNA therapeutics. *Nat. Nanotechnol.* 16(9), 1030–1038 (2021).
11. Lee H, Odom TW. Controlling ligand density on nanoparticles as a means to enhance biological activity. *Nanomedicine* 10(2), 177–180 (2015).
12. Herrera-Barrera M, Ryals RC, Gautam M *et al.* Peptide-guided lipid nanoparticles deliver mRNA to the neural retina of rodents and nonhuman primates. *Sci. Adv.* 9, eadd4623 (2023).
13. Cui L, Pereira S, Sonzini S *et al.* Development of a high-throughput platform for screening lipid nanoparticles for mRNA delivery. *Nanoscale* 14(4), 1480–1491 (2022).
14. Chen C, Zhou Y, Chen C, Zhu S, Yan X. Quantification of available ligand density on the surface of targeted liposomal nanomedicines at the single-particle level. *ACS Nano* 16(4), 6886–6897 (2022).

•• **Reported there is an optimal ligand density of nanoparticles for cell targeting.**

15. Li H, Di J, Peng B, Xu Y, Zhang N. Surface ligand valency and immunoliposome binding: when more is not always better. *Pharm. Res.* 38(9), 1593–1600 (2021).

•• **Reported how feed ratio of functional ligands influenced targetability.**

16. Hirata Y, Tashima R, Mitsuhashi N *et al.* A simple, fast, and orientation-controllable technology for preparing antibody-modified liposomes. *Int. J. Pharm.* 607, 120966 (2021).
17. Woll S, Bachran C, Schiller S *et al.* Sortagging of liposomes with a murine CD11b-specific VHH increases *in vitro* and *in vivo* targeting specificity of myeloid cells. *Eur. J. Pharm. Biopharm.* 134, 190–198 (2019).
18. Shim G, Kim D, Lee S, Chang RS, Byun J, Oh YK. *Staphylococcus aureus*-mimetic control of antibody orientation on nanoparticles. *Nanomedicine* 16, 267–277 (2019).

• **Reported how to control the orientation of antibody that was conjugated on the surface of nanoparticles.**

19. Maeki M, Saito T, Sato Y *et al.* A strategy for synthesis of lipid nanoparticles using microfluidic devices with a mixer structure. *RSC Adv.* 5(57), 46181–46185 (2015).
20. Kulkarni JA, Darjuan MM, Mercer JE *et al.* On the formation and morphology of lipid nanoparticles containing ionizable cationic lipids and siRNA. *ACS Nano* 12(5), 4787–4795 (2018).
21. Benchimol MJ, Hsu MJ, Schutt CE *et al.* Phospholipid/carbocyanine dye-shelled microbubbles as ultrasound-modulated fluorescent contrast agents. *Soft Matter* 9(8), 2384–2388 (2013).
22. Ren WX, Han J, Uhm S *et al.* Recent development of biotin conjugation in biological imaging, sensing, and target delivery. *Chem. Commun.* 51(52), 10403–10418 (2015).
23. Takayama Y, Kusamori K, Tsukimori C *et al.* Anticancer drug-loaded mesenchymal stem cells for targeted cancer therapy. *J. Control. Rel.* 329, 1090–1101 (2021).

• **Reported how to use biotin-LNP to target cancers.**

24. Medina LA, Calixto SM, Klipper R, Phillips WT, Goins B. Avidin/biotin-liposome system injected in the pleural space for drug delivery to mediastinal lymph nodes. *J. Pharm. Sci.* 93(10), 2595–2608 (2004).

• **Reported how to use biotin/avidin system for targeted drug delivery.**

25. Ferhan AR, Park S, Park H, Tae H, Jackman JA, Cho NJ. Lipid nanoparticle technologies for nucleic acid delivery: a nanoarchitectonics perspective. *Adv. Funct. Mater.* 32(37), 2203669 (2022).
26. Bandara SR, Molley TG, Kim H *et al.* The structural fate of lipid nanoparticles in the extracellular matrix. *Mater. Horiz.* 7(1), 125–134 (2020).
27. Sakuragi M, Koiwai K, Nakamura K *et al.* Transformation from multilamellar to unilamellar vesicles by addition of a cationic lipid to PEGylated liposomes explored with synchrotron small angle x-ray scattering. *J. Phys.Conf. Ser.* 272, 1–10 (2011).